# A novel function for the atypical small G protein Rab-like 5 in the assembly of the trypanosome flagellum

**Christine Adhiambo[1], Thierry Blisnick[1], Géraldine Toutirais[2], Emmanuelle Delannoy[2] and Philippe Bastin[1,*]**

[1]Trypanosome Cell Biology Unit, Pasteur Institute and CNRS, Paris, France
[2]Dynamique et Régulation des Génomes, Muséum National d'Histoire Naturelle, INSERM and CNRS, Paris, France
*Author for correspondence (e-mail: philippe.bastin@pasteur.fr)

*Accepted 7 November 2008*
*Journal of Cell Science 122, 834-841 Published by The Company of Biologists 2009*
*doi:10.1242/jcs.040444*

## Summary

**The atypical small G protein Rab-like 5 has been shown to traffic in sensory cilia of *Caenorhabditis elegans*, where it participates in signalling processes but not in cilia construction. In this report, we demonstrate that RABL5 colocalises with intraflagellar transport (IFT) proteins at the basal body and in the flagellum matrix of the protist *Trypanosoma brucei*. RABL5 fused to GFP exhibits anterograde movement in the flagellum of live trypanosomes, suggesting it could be associated with IFT. Accordingly, RABL5 accumulates in the short flagella of the retrograde *IFT140*$^{RNAi}$ mutant and is restricted to the basal body region in the *IFT88*$^{RNAi}$ anterograde mutant, a behaviour that is identical to other IFT proteins. Strikingly, RNAi silencing reveals an essential role for RABL5 in trypanosome flagellum construction. RNAi knock-down produces a phenotype similar to inactivation of retrograde IFT with formation of short flagella that are filled with a high amount of IFT proteins. These data reveal for the first time a functional difference for a conserved flagellar matrix protein between two different ciliated species and raise questions related to cilia diversity.**

Supplementary material available online at
http://jcs.biologists.org/cgi/content/full/122/6/834/DC1

Key words: G-protein, RAB-Like, Intraflagellar transport, Flagella, Cilia, *Trypanosoma brucei*

## Introduction

The basic structure of cilia and flagella is the axoneme, a set of nine doublet microtubules organised in a cylindrical manner with (9+2) or without (9+0) a central pair of microtubules. Dynein arms and radial spokes are involved in generation and control of beating and are mostly found on 9+2 axonemes (Ralston and Hill, 2008). Ciliary microtubules originate and extend from the basal body, a cytoplasmic centriolar-like structure that is usually composed of nine triplet microtubules. During cilium construction, proteins are added at the distal tip of the elongating organelle by a process called intraflagellar transport (IFT) (Rosenbaum and Witman, 2002). IFT is defined as the bidirectional movement of protein complexes from the base of the cilia to the distal tip (anterograde transport, powered by heterotrimeric kinesin II) and back towards the cell body (retrograde transport, driven by a specific dynein complex). IFT complex A (at least six polypeptides) and complex B (at least 11 polypeptides) (Cole et al., 1998) are required for retrograde and anterograde IFT, respectively. IFT proteins and their functions are conserved in all flagellated species examined so far: algae, nematodes, insects, trypanosomes, ciliates and mammals (Kohl and Bastin, 2005). These IFT proteins are rich in protein-protein interaction domains such as WD40 and tetratricopeptide repeats (TPR) or coiled-coils (Cole, 2003). One of few exceptions is the small G protein IFT27 (RAB-like 4), which is part of the B complex and is required for flagellum formation in *Chlamydomonas* (Cole et al., 1998; Qin et al., 2007). Other small G proteins have been shown to participate to formation of cilia and flagella such as ARL3 in *Leishmania* (Cuvillier et al., 2000), ARL6 [a protein that is mutated in some individuals who suffer from the Bardet-Biedl syndrome, a cilia-related disease (Fan et al., 2004)] and Rab8 in mammalian cells (Omori et al., 2008).

Rab-like 5 (RABL5 or IFTA-2 in *C. elegans*) is an atypical G protein that lacks the G4 domain of the GTP-binding region and the prenylation motif. The protein has been localised to the basal body and the ciliary compartment in *C. elegans* sensory neurons and to the primary cilium of inner medullary collecting duct (IMCD) cells or of retinal pigmented epithelial (RPE1) cells (Schafer et al., 2006; Yoshimura et al., 2007). RABL5 fused to GFP is transported in the nematode cilia but RABL5 inactivation in two independent deletion mutants did not result in visible alteration of ciliary structure, nor in perturbation of sensory perception in the mutant worms. However, an extended lifespan phenotype was observed and was linked to defects in DAF2/insulin/IGF-like 1 signalling pathway, leading to the suggestion that RABL5 is involved in sensing rather than in axoneme construction (Schafer et al., 2006).

Using comparative genomics of species assembling flagella with or without IFT, we and others have identified several genes that are restricted to organisms assembling their flagella by IFT (putatively involved in intraflagellar transport or PIFT) (Absalon et al., 2008b; Avidor-Reiss et al., 2004; Briggs et al., 2004; Li et al., 2004). The *RABL5* gene was found to belong to this category, suggesting a function related to IFT. However, it could not be identified in insect genomes such as *Drosophila* or *Anopheles*, despite the fact that cilia in their sensory neurons (9+0) are assembled by IFT. If RABL5 is involved in sensing functions (Schafer et al., 2006), its exact role remains to be determined as it is present in organisms with very different types of cilia and the range of signals that these cilia might have to detect are likely to diverge extensively. We therefore investigated the role of RABL5 in a different organism: the protist *Trypanosoma brucei*. This micro-organism possesses a single flagellum with a classic motile 9+2 axoneme and has become an attractive model for functional

studies (Baron et al., 2007; Broadhead et al., 2006; Kohl and Bastin, 2005; Ralston and Hill, 2008). The trypanosome RABL5 was found to localise to the flagellum and basal body compartments, where it demonstrated the characteristics of an IFT protein similar to that observed in *C. elegans*. However, knocking-down RABL5 by RNAi resulted in the formation of very short flagella that were filled with IFT-like material. These data, thus, reveal a novel function for RABL5 in retrograde IFT. In contrast to the well-conserved function of IFT proteins in flagellum construction, RABL5 is the first matrix ciliary protein to show radically different roles between two ciliated/flagellated organisms.

## Results

### RABL5 encodes a putative Rab-like protein and is restricted to certain ciliated species

The *RABL5* gene (GeneDB Accession Number, Tb11.01.8590) is 660 nucleotides long and encodes a predicted protein of 219 amino acids long with a calculated molecular mass of 24.4 kDa and an iso-electric point of 5.2. Classification of RABL5 as a putative Rab protein is based on BLAST searches and on sequence alignment of the G-domains found in most Rab proteins and involved in GTP/GDP binding. The first three G-domains of the five Ras GTPase consensus sequences are well-conserved in all the RABL5 sequences examined (Fig. 1). By contrast, a conventional G4 box is not present in all the RABL5 analysed, whereas the G5 box shows more diversity. None of the RABL5 proteins exhibits the consensus sequence E(T/G/S)(G/S)A, the closest match being found in Trypanosomatids (*T. brucei*, *T. cruzi*, *Leishmania major*, *L. braziliensis* and *L. infantum*). In these five species, the consensus sequence is ETSL. A variation in the consensus sequence is found in two other protists: DTSI in both *Paramecium* orthologues and KTSM in *Giardia lamblia*. All vertebrate RABL5 sequences display the sequence HSNL (human, mouse, rat, dog, cow, opossum and fish), whereas the most divergent sequences are found in *Chlamydomonas* (AINP) or *Caenorhabditis* (AAHF) species and do not fit with the consensus. The *C. elegans* sequence contains two insertions of 23 and 25 amino acids before and after the G1 domain, respectively, making it the longest of the RABL5 sequences identified (252 amino acids compared with 185-219 amino acids for the others). The Trypanosomatid RABL5 proteins are slightly larger than their vertebrate counterpart owing to the insertion of six amino acids between the G1 and G2 domains and 10 amino acids between the G3 and the G5 domains. Additionally, it possesses a longer C-terminal extension. The prenylation domain CCxx xCCx, which is usually located at the C-terminal end of the Rab proteins, is missing, indicating that they are unlikely to be lipid modified. A clear homologue of RABL5 was found in all ciliated/flagellated organisms except in *Drosophila* and *Anopheles*. Like all the well-characterised *IFT* genes, *RABL5* is missing from the genome of *Plasmodium falciparum*, a parasite that assembles its flagella in the cytoplasm (Briggs et al., 2004). Finally, BLAST analysis demonstrated that RABL5 proteins are clearly distinct from all other RAB families, including RABL4/IFT27 (*T. brucei* RABL4 and RABL5 are less than 15% identical).

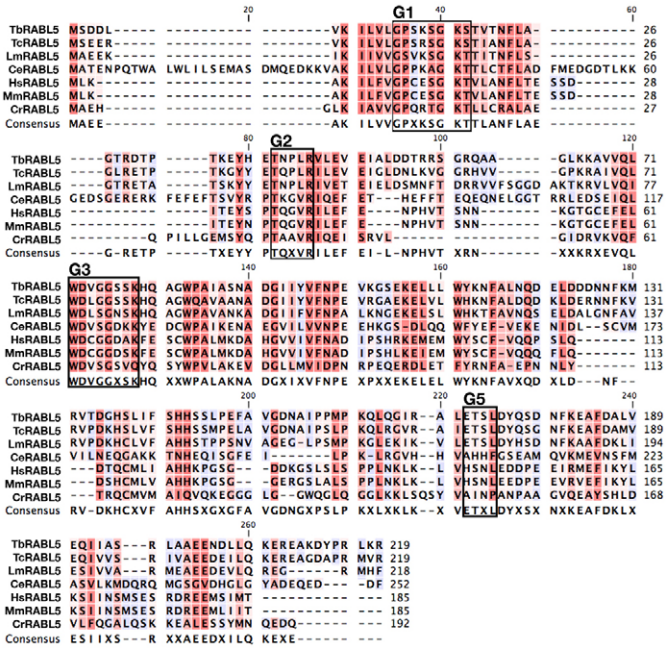


**Fig. 1.** Alignment of deduced amino acid sequences of RABL5 homologues. Alignment was generated using ClustalW; the most conserved residues are shown in red, the less conserved in blue. G1-G5 indicates conserved motifs implicated in nucleotide binding domains. Dashes indicate gaps introduced to optimize the alignment. Consensus indicates where the majority of residues match. Abbreviations and GenBank Accession Numbers of predicted protein sequences are as follows: Tb (*Trypanosoma brucei*), EAN80628/Tb11.01.8590; Tc (*Trypanosoma cruzi*), EAN83652; Lm (*Leishmania major*), CAJ08852; Ce (*Caenorhabditis elegans*), NP_503073; Hs (*Homo sapiens*), NP_073614; Mm (*Mus musculus*), AAH09150; Cr (*Chlamydomonas reinhardtii*), XP_001689669.1.

### RABL5 is localised at the basal body and the flagellum matrix

To determine the location of the trypanosome RABL5, the full-length RABL5 was fused to glutathione-S-transferase (GST), expressed in bacteria, purified and injected into mice to generate polyclonal antibodies. Control mice were immunized with GST alone and sera were adsorbed against GST prior to being used for western blotting. In wild-type cells, the antibody detected a single band migrating close to the 25 kDa marker, i.e. in the range of the expected molecular weight of RABL5 (Fig. 2A, arrow). In cells expressing a GFP::RABL5 fusion protein, a supplementary band of $M_r$ ~50 K was visible, which is comparable with the predicted mass of the fusion protein (Fig. 2A, star; and see below). The anti-RABL5 antiserum was used in indirect immunofluorescence assay (IFA) in combination with the monoclonal antibody MAb25 that stains exclusively a cytoskeletal component of the axoneme (Absalon et al., 2007; Pradel et al., 2006) to reveal the flagellum (Fig. 2B, arrows), and with DAPI to stain DNA in the nucleus and the mitochondrial genome (kinetoplast). The kinetoplast is physically linked to the basal body of the flagellum and hence is a good indicator of basal body position (Robinson and Gull, 1991). Trypanosomes maintain their existing flagellum while growing a new one; hence, cells can be found with one (Fig. 2B, lower cell) or two flagella (upper cells at Fig. 2B). The new flagellum (Fig. 2B, yellow arrows) can easily be identified as it is always positioned at the wider, posterior, end of the cell (Sherwin and Gull, 1989). The anti-RABL5 antiserum decorated equally both old and new flagella but the labelling was discontinuous and slightly shifted from the central axis of the flagellum when compared with that observed for MAb25 (Fig. 2B, merged panel). The anti-RABL5 signal extended to the basal body region where it often appeared brighter (Fig. 2B, arrowheads). By contrast, only a weak cytoplasmic background labelling was produced using the control anti-GST (data not shown). We also generated trypanosomes expressing GFP-

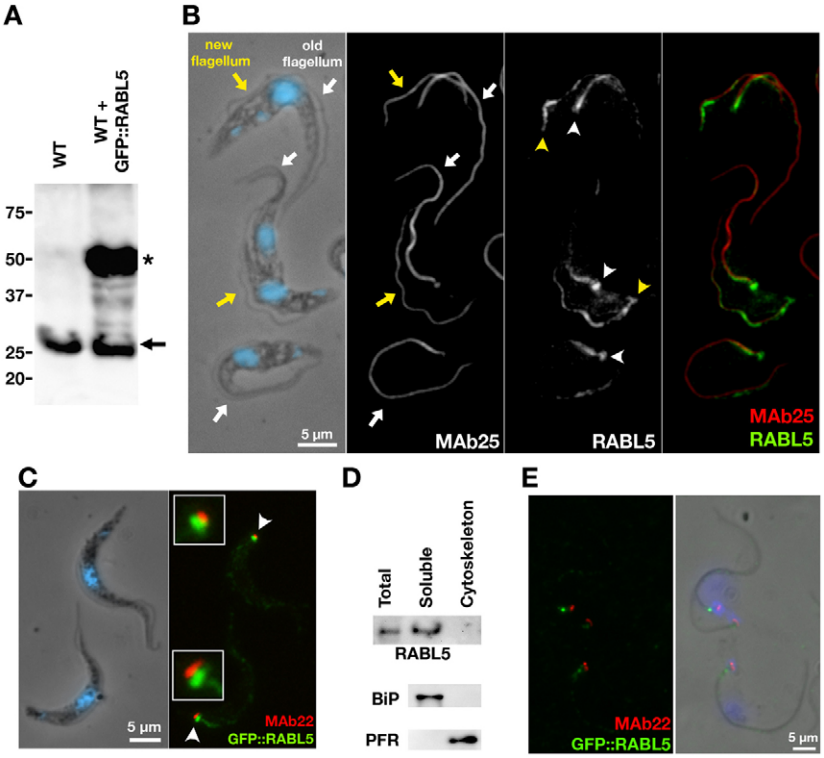


**Fig. 2.** RABL5 is associated with the basal body and the flagellum matrix. (A) Western blot of total protein samples showing expression of RABL5 at its expected $M_r$ (arrow) in wild-type cells (WT) and the presence of an additional band (*) corresponding to the GFP::RABL5 in wild-type cells transfected with pPCPFReGFPRABL5 (WT+GFP::RABL5). (B) Wild-type cells fixed in methanol double-stained with the anti-axoneme marker MAb25 and the anti-RABL5 antiserum as indicated. The first panel shows the phase-contrast image merged with DAPI staining (blue) to visualise nuclear and kinetoplast DNA. Arrows indicate the flagella and arrowheads indicate basal body staining. New flagella and basal bodies are shown in yellow and old ones are shown in white. (C) GFP::RABL5 (green) -expressing trypanosomes fixed in methanol and stained with the basal body marker MAb22 (red) and with DAPI (blue). The basal body regions (arrowheads) are magnified (insets). The merged image (right) reveals that RABL5 stains the distal region of the basal body. (D) Wild-type trypanosomes were washed and treated with Nonidet P-40 1% to extract the cytoskeleton from the detergent soluble fraction. Protein samples were separated by SDS-PAGE, transferred to membranes and incubated with the indicated antibodies. The endoplasmic reticulum protein BiP was taken as marker of the soluble fraction and the paraflagellar rod (PFR) proteins were used as markers of the cytoskeleton. Most of the RABL5 protein pool is found in the soluble fraction. (E) The same treatment was applied to GFP::RABL5-expressing cells and analysed by IFA using MAb22 to reveal the fibres linked to the proximal basal body. GFP::RABL5 is still present at the basal body but cytoplasmic and flagellar staining are lost.

tagged RABL5 in a wild-type background. On both live and fixed cells, GFP::RABL5 localised to the cytoplasm, basal body and flagellum (Fig. 2C; data not shown), i.e. a similar pattern to the results from IFA experiments where cells were probed with the anti-RABL5 and further supports an association of RABL5 with the flagellum and basal body compartments.

To investigate the localisation pattern linked to the basal body, we performed double IFA labelling with MAb22, a monoclonal antibody marker of the fibres that link the proximal part of both the mature and pro-basal body to the kinetoplast (Bonhivers et al., 2008). In all cells, the MAb22 and the RABL5 (with the antibody or the GFP fusion) signals exhibited close but clearly different locations, with RABL5 being always on the most distal region of the basal body (Fig. 2C), a localisation similar to that of the three known IFT proteins in trypanosomes (Absalon et al., 2008b). To further establish the association of RABL5 with the IFT particles, detergent treatment was applied to trypanosomes, a procedure that removes the cell membrane and extracts an intact cytoskeleton (Sherwin and Gull, 1989), including the flagellum (Broadhead et al., 2006). Under these conditions, RABL5 fractionated with the soluble fraction, similar to the endoplasmic reticulum control marker BiP and in contrast to cytoskeletal proteins such as the PFR (Fig. 2D). Analysis of cytoskeletons by IFA showed that RABL5 (data not shown) or the GFP::RABL5 fusion protein (Fig. 2E) only remained associated to the basal body upon detergent treatment, whereas the flagellum and cell body signal was abolished, as reported previously for IFT proteins (Absalon et al., 2008b). The absence of RABL5 in the cytoskeletal fraction probably reflects the low amount of proteins present at the basal body compared with the flagellum and the cell body.

To firmly establish the association between IFT proteins and RABL5, double IFA staining was performed with antibodies against IFT172 (involved in anterograde transport, Fig. 3A) or against PIFTF6/IFT144 (involved in retrograde transport, Fig. 3B) (Absalon et al., 2008b). A close but not exact colocalisation of the RABL5 signal at the basal body and within the flagellum matrix was observed in both experiments (Fig. 3A,B). Taken together, these results suggest that RABL5 could be associated to IFT.

### RABL5 traffics in the flagellum and is sensitive to loss of IFT

Trypanosomes expressing GFP::RABL5 were used to visualise the possible movement of RABL5 in the flagellum of live cells. Clear intraflagellar movement of GFP::RABL5 was detected, mainly from the base of the flagellum to the tip (anterograde movement) (Fig. 4A; supplementary material Movie 1). As observed for GFP::IFT52 in trypanosomes (Absalon et al., 2008b) or with GFP::IFT20 in mammalian primary cilia (Follit et al., 2006), retrograde events were more difficult to visualise. We next investigated the behaviour of GFP::RABL5 in cell lines where IFT had been perturbed. First, when retrograde IFT is blocked, trypanosomes assemble short flagella filled with IFT particles that cannot be recycled to the basal body region (Absalon et al., 2008b). Whereas RABL5 exhibited the usual basal body and flagellum signals in non-induced cells (Fig. 4B), it accumulated in the short flagella of the *IFT140*$^{RNAi}$ mutant in every cell examined (Fig. 4C,D). All the IFT proteins examined to date accumulate in the short flagella of retrograde transport mutants, in contrast to the proteins from the axoneme or the PFR (Absalon et al., 2008b). Inhibition of anterograde movement in the *IFT88*$^{RNAi}$ mutant prevents flagellum formation. Under these conditions, RABL5 was found only at the basal body and accumulation of large amounts of material was not observed (Fig. 4E). These data demonstrate that RABL5 exhibits intraflagellar movement in live cells and behaves like the IFT proteins both in normal cells and in retrograde and anterograde IFT mutants.

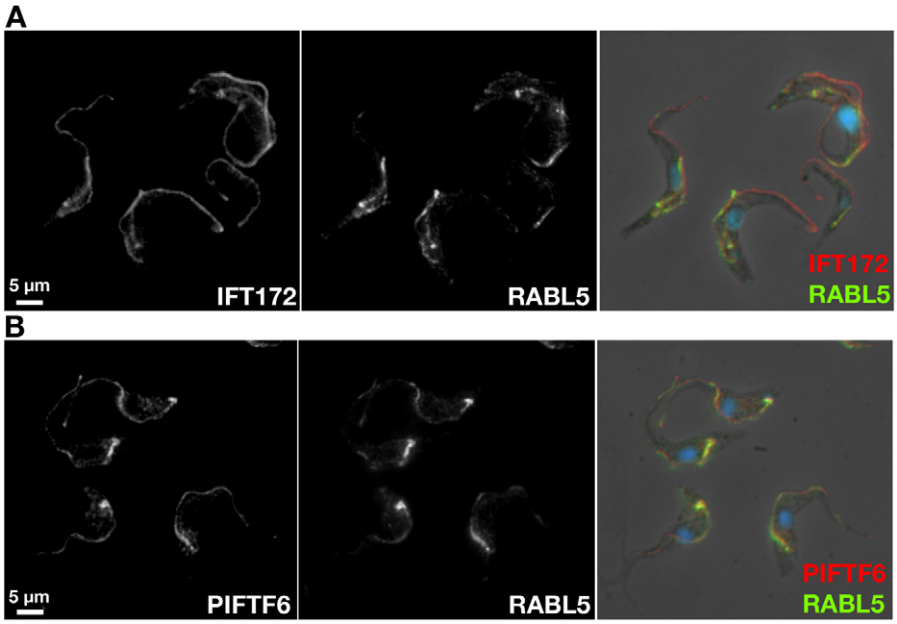


**Fig. 3.** RABL5 shows close colocalisation with IFT proteins. Wild-type cells fixed in methanol were stained with the anti-RABL5 antiserum and (A) with antibodies against IFT172, a protein required for anterograde transport, or (B) with PIFTF6/IFT144, a protein required for retrograde transport, as indicated. The left panels show the anti-IFT172 (A) or anti-PIFTD6 (B) signal, the middle panels show the RABL5 signal and the merged fluorescent images with the corresponding phase and DAPI (blue) images are shown in the right panels.

### Silencing of RABL5 in trypanosomes results in flagellar assembly defects similar to inhibition of retrograde IFT

Tetracycline-inducible RNA interference (RNAi) was used to deplete RABL5 and examine its functions in trypanosomes. RT-PCR confirmed that *RABL5* mRNA was rapidly degraded upon induction of RNAi silencing, whereas the level of mRNA for aldolase used as control was not affected (Fig. 5A). Western blot analysis using the anti-RABL5 polyclonal antibody showed that the endogenous RABL5 dropped rapidly and became barely detectible 2 days after induction (Fig. 5B). *RABL5*$^{RNAi}$ cells grew normally for 4 days until they stopped proliferating and died (Fig. 5C). Examination of cells 3-4 days after induction revealed the emergence of short cells that were typical of inhibition of flagellum formation (Absalon et al., 2008b; Absalon et al., 2007; Kohl et al., 2003) (Fig. 5D). IFA with the axoneme marker MAb25 revealed that *RABL5*$^{RNAi}$ cells induced for 4 days assemble abnormally short flagella (Fig. 5D), the average length of which was 3.1±1.4 μm ($n$=50) instead of 18.5±2.9 μm ($n$=50) for non-induced controls. Trypanosomes assemble a new flagellum while maintaining the existing one (Fig. 5E) and scanning electron microscopy revealed that *RABL5*$^{RNAi}$ cells induced for 3 or 4 days still possessed an apparently intact old flagellum (Fig. 5F,G, white arrows) but assembled a very short new flagellum (yellow arrows). After cytokinesis, the cell inheriting the short new flagellum was too small and its flagellum did not show signs of further elongation (Fig. 5H,I, arrows). Supplementary membrane-like extensions were frequently observed (Fig. 5F-J, arrowheads), presumably corresponding to the 'flagellar sleeve' reported in other IFT mutants in trypanosomes (Absalon et al., 2008b; Davidge et al., 2006). Some cells were also observed without a flagellum but structures resembling vesicles could be recognised emerging from the flagellar pocket area (Fig. 5J).

This phenotype strongly resembles that observed upon inhibition of retrograde IFT. This inhibition leads to formation of short flagella filled with IFT proteins but these proteins cannot be recycled to the cell body (Blacque et al., 2006; Pazour et al., 1999; Porter et al., 1999; Signor et al., 1999). We therefore analysed the location of IFT proteins in *RABL5*$^{RNAi}$ cells. IFA with the anti-IFT172 antiserum revealed normal staining in non-induced cells (Fig. 6A), whereas clear accumulation of IFT172 in the short flagella of *RABL5*$^{RNAi}$ cells induced for 4 days was striking (Fig. 6B). Quantitative analysis confirmed the presence of a large proportion of these cells similar to retrograde *IFT140*$^{RNAi}$ or *DHC1b*$^{RNAi}$ cells, but in contrast to the anterograde *IFT88*$^{RNAi}$ mutant (Fig. 6C).

To analyse the nature of the material accumulated in the short flagella of *RABL5*$^{RNAi}$ trypanosomes, we examined these cells by transmission electron microscopy. Whereas control samples presented the normal aspect of the basal body and the flagellum emerging from the flagellar pocket (Fig. 7A), *RABL5*$^{RNAi}$ cells exhibited bulbous short flagella filled with IFT-like material, a feature typical of cells with defective retrograde transport (Fig. 7B,C). Quantitative analysis revealed that 59% of the sections through flagella of the *RABL5*$^{RNAi}$ mutant cells showed clear accumulation of IFT material ($n$=27), a proportion similar to that observed for the retrograde transport mutants *DHC1b*$^{RNAi}$ (35%, $n$=48) and *IFT140*$^{RNAi}$ (45%, $n$=38). By contrast, no accumulation of IFT-like material could be detected in the short flagellar stubs of the anterograde transport mutants *IFT88*$^{RNAi}$ (0%, $n$=23) and *IFT172*$^{RNAi}$ (0%, $n$=28). Furthermore, *RABL5*$^{RNAi}$ cells also exhibited all the typical phenotypes that resulted from defects in flagellum formation: inhibition of cytokinesis, growth arrest and multiple rounds of basal body duplication that fail to migrate and also defects in formation of the flagellar pocket (supplementary material Fig. S1; data not shown) (Absalon et al., 2008a; Absalon et al., 2008b; Absalon et al., 2007; Davidge et al., 2006; Kohl et al., 2003).

## DISCUSSION

### RABL5 is localised at the basal body and flagellum matrix where it undergoes IFT

The endogenous RABL5 or the fusion protein GFP::RABL5 show a clear localisation to the basal body and the flagellum matrix. This pattern is very similar to what was observed for IFT proteins such as IFT20, IFT52 and IFT172 (Absalon et al., 2008b). The GFP::RABL5 fusion protein is transported in the flagellum matrix and behaves similarly to the GFP::IFT52 protein (Absalon et al.,

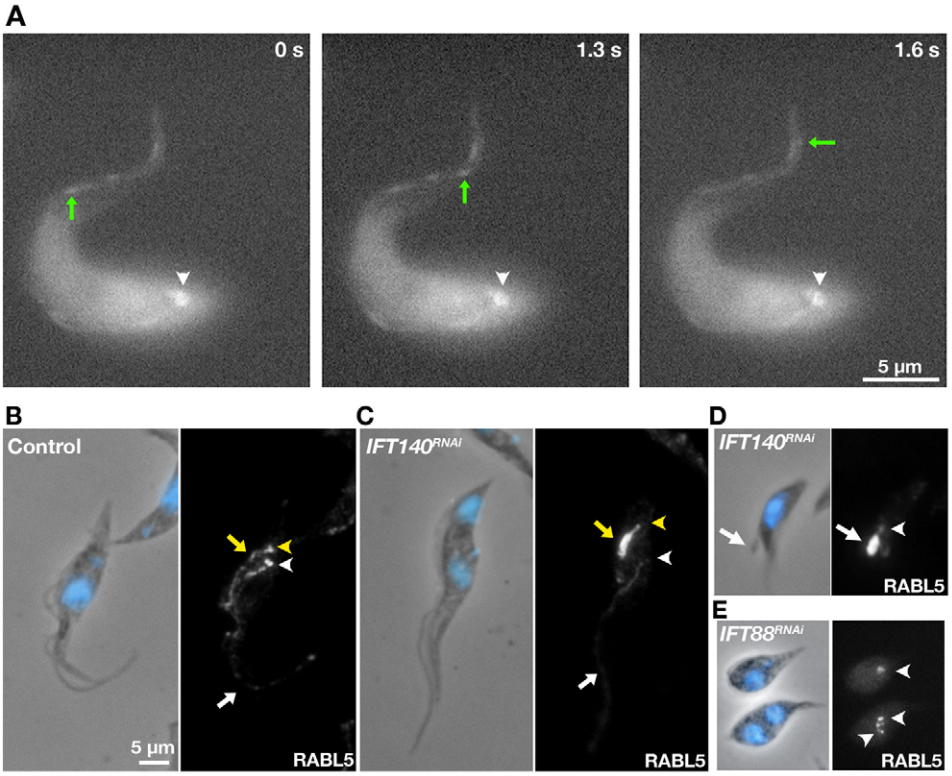


**Fig. 4.** RABL5 is linked to IFT. (A) GFP::RABL5 moves in the trypanosome flagellum. Still images of Movie 1 (supplementary material) are shown (elapsed time in seconds). The green arrow indicates a moving fluorescent particle and the white arrowhead shows the basal body. (B-E) Non-induced (B), *IFT140*$^{RNAi}$ (C,D) or *IFT88*$^{RNAi}$ (E) cells induced for 2 days stained with the anti-RABL5 antiserum as indicated. Arrows show flagella and arrowheads indicate basal bodies. New flagella and basal bodies are shown in yellow and old ones are shown in white. Clear accumulation of RABL5 in the short flagella of *IFT140*$^{RNAi}$ cells is detected (C,D), whereas only basal body signal is found in *IFT88*$^{RNAi}$ cells (E). B-E are at the same magnification.

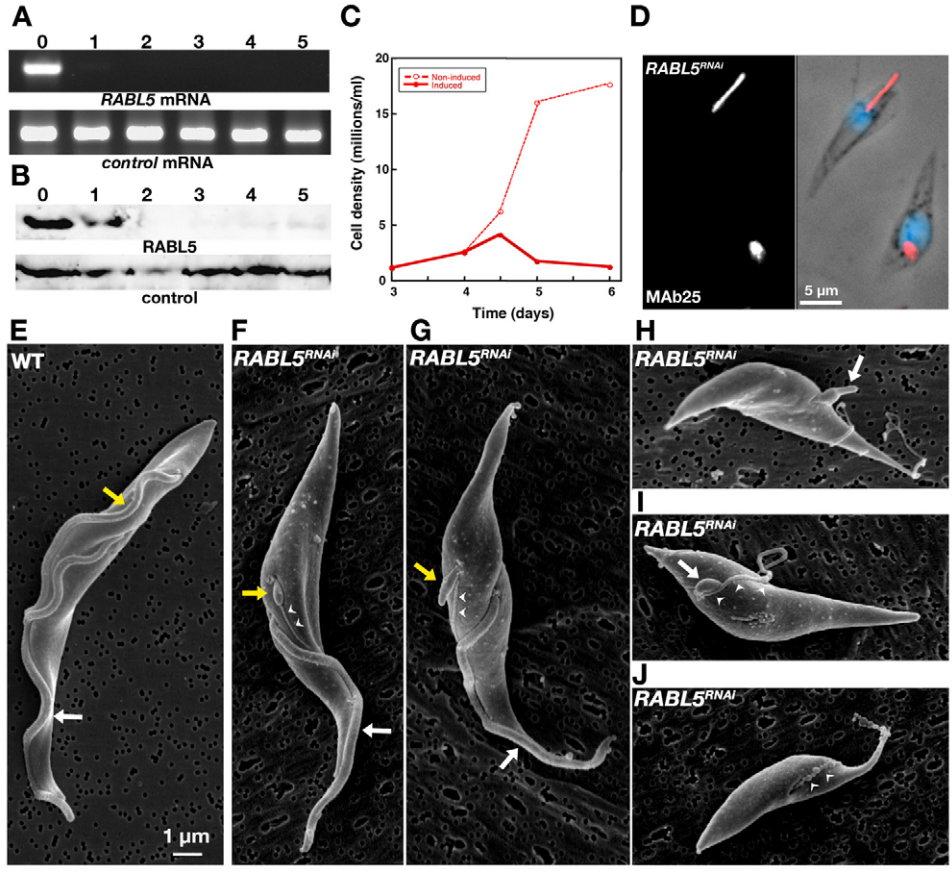


**Fig. 5.** Silencing of RABL5 perturbs flagellum assembly. (A) RT-PCR performed on total RNA from non-induced and *RABL5*$^{RNAi}$ cells induced for the indicated number of days shows potent silencing of the *RABL5* mRNA. Aldolase was used as control. (B) Western blot showing the effect of RNAi silencing on the endogenous RABL5 protein. Total protein extract (20 µg) from non-induced and *RABL5*$^{RNAi}$ cells induced for the indicated number of days were run on a gel, transferred to a membrane and incubated with the anti-RABL5 or the anti-Bip as loading control. (C) Growth curve of non-induced (thin line) and induced (thick line) *RABL5*$^{RNAi}$ cells. (D) *RABL5*$^{RNAi}$ cells induced for 4 days stained with the anti-axoneme MAb25 (red) and with DAPI (blue), showing the presence of unusually short flagella. (E-J) Scanning electron micrographs of wild-type or *RABL5*$^{RNAi}$ cells induced for 4 days (same scale). An old (white arrow) and a new (yellow arrow) flagellum can be seen on control cells (E), whereas only a short new flagellum is constructed by the *RABL5*$^{RNAi}$ cells (F,G). (H-J) Daughter cells inheriting the short flagellum (white arrow). Arrowheads indicate membrane extensions or vesicles emerging from the flagellar pocket.

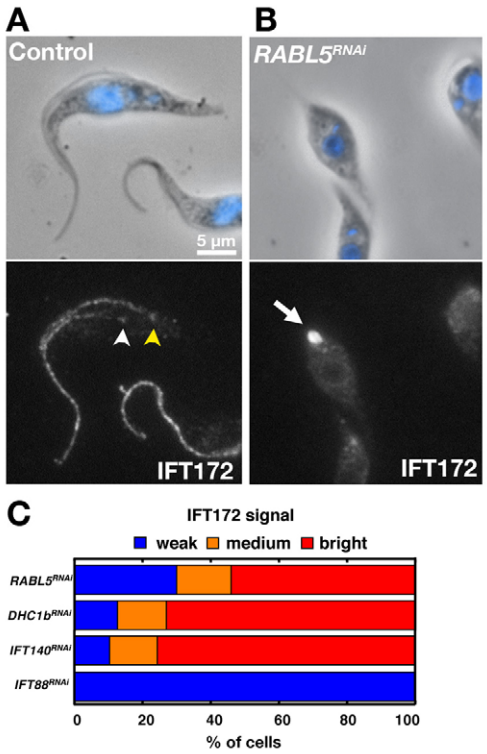


**Fig. 6.** *RABL5*$^{RNAi}$ assemble short flagella accumulating IFT proteins like retrograde IFT mutants. *RABL5*$^{RNAi}$ cells were non-induced (A) or induced for 4 days (B), labelled with the anti-IFT172 and counterstained with DAPI (blue). Arrow shows the accumulation of IFT proteins in the short flagellum (same scale). Arrowheads indicate the position of old (white) and new (yellow) basal bodies. (C) Cells were induced for 4 (*RABL5*$^{RNAi}$) or 3 days (*DHC1b*$^{RNAi}$, *IFT140*$^{RNAi}$ and *IFT88*$^{RNAi}$), and stained with the anti-IFT172 antiserum. The proportion of short cells displaying no, weak or bright signal ($n \geq 100$) is shown. *RABL5*$^{RNAi}$ typically behaves like the other IFT retrograde transport mutants described above.

2008b). These results are in agreement with the presence of RABL5 in sensory cilia of *C. elegans* where it also undergoes IFT (Ou et al., 2007; Schafer et al., 2006). At least two functions can be considered for RABL5: (1) it is a cargo transported by the IFT particles; or (2) it is an integral component of the IFT particle. In *Chlamydomonas*, RABL5 (FAP9) has been found in the flagellum matrix (Pazour et al., 2005) and its mRNA is upregulated upon deflagellation (Li et al., 2004), similar to the expression profile of other flagellar proteins. By contrast, RABL5 is not associated to the cytoskeletal fraction of the flagellum, neither in the green algae (Pazour et al., 2005), nor in trypanosomes (Broadhead et al., 2006). Finally, RABL5 was not found among the proteins present in IFT particles purified from *Chlamydomonas* (Cole, 2003).

In mammalian cells, RABL5 has been localised to the basal body and the ciliary compartment of the primary cilium in inner medullary collecting duct (IMCD) cells or in retinal pigmented epithelial (RPE1) cells (Schafer et al., 2006; Yoshimura et al., 2007). It has also been found at the Golgi level in non-ciliated NIH3T3 cells (Yang et al., 2007). Intriguingly, we noticed that in trypanosome cells overexpressing large amounts of GFP::RABL5, the protein was consistently found at the Golgi apparatus in addition to the flagellum and basal body (data not shown). It is difficult to establish whether this localisation is the result of overexpression of the fusion protein or whether the absence of RABL5 at the Golgi level in wild-type cells is due to a lack in sensitivity of the anti-RABL5 antibody. In several mammalian cell lines, IFT20 is present at the Golgi apparatus in addition to the basal body and the matrix of the flagellum, suggesting it might function in the delivery of flagellar membrane proteins (Follit et al., 2006). However, this was not observed in trypanosomes where IFT20 is exclusively localised to the flagellum and the basal body (Absalon et al., 2008b).

### RABL5 is required for flagellum formation and could participate to retrograde IFT

RNAi knock-down demonstrates that RABL5 is required for flagellum formation and produces a phenotype typical of defects in retrograde IFT, similar to those observed upon silencing of IFT122, IFT140 (Absalon et al., 2008b) or the retrograde transport motor DHC1b (Kohl et al., 2003). This phenotype supports the hypothesis that RABL5 is part of the IFT particle or somehow regulates its function. It is possible that RABL5 association with the IFT particle(s) is less stable or only transient, or its stoichiometry is lower compared with the other IFT component proteins identified thus far. Interestingly, a better colocalisation of RABL5 has been obtained with PIFTF6/IFT144 (required for retrograde IFT) compared with IFT172 (required for anterograde IFT). However, this could also be due to the access of antibodies to their target, especially if these proteins are part of large complexes as observed in the green algae *Chlamydomonas*. In any case, this situation is in stark contrast to *C. elegans*, where RABL5 demonstrates IFT but is not required for formation of cilia (Schafer et al., 2006). RABL5 is the first reported matrix ciliary protein that performs such drastically different functions between two organisms. In molecular terms, this difference in function could be related to sequence divergences. For example, the *C. elegans* RABL5 protein possesses two long insertions that are not found in other species and does not contain a G5 domain, in contrast to Trypanosomatids where three out of four residues of the G5 box are conserved. At the biological level, one possible explanation could come from the different types of cilia between trypanosomes and nematodes. *C. elegans* possesses 9+0 non-motile cilia, whereas *T. brucei* possesses a 9+2 motile flagellum that contains a central pair, dynein arms and radial spokes. These multi-protein complexes are transported by IFT (Piperno et al., 1996; Qin et al., 2004) and this requirement could modify the organisation of the periphery of the IFT particles. If RABL5 is positioned differently in the IFT particle in various types of cilia, its absence could have different consequences on IFT and flagellum formation. Understanding the exact role of RABL5 will require knowledge of the biochemistry of the IFT particles that is not yet available neither for *T. brucei* nor for *C. elegans*.

Despite their well-conserved structure, cilia and flagella have become specialised to fulfill variable functions. The best example is found in mammals, where multiple types of cilia are present: motile 9+2 cilia in the respiratory epithelium, motile 9+0 cilia at the embryonic node, non-motile 9+0 primary cilia, the connecting cilium of photoreceptors or the motile sperm flagellum all have different organisations and roles. It was long-assumed that the function of IFT proteins was fully conserved in different cilia, but recent data show subtle differences for motor or IFT proteins in *C. elegans* or in zebrafish (Krock and Perkins, 2008; Mukhopadhyay et al., 2007; Scholey, 2008). This diversity could be especially important in complex genetic diseases related to defects in cilia and flagella such as in the Bardet-Biedl syndrome (Marshall, 2008). Extensive symptom diversity between individuals has been reported

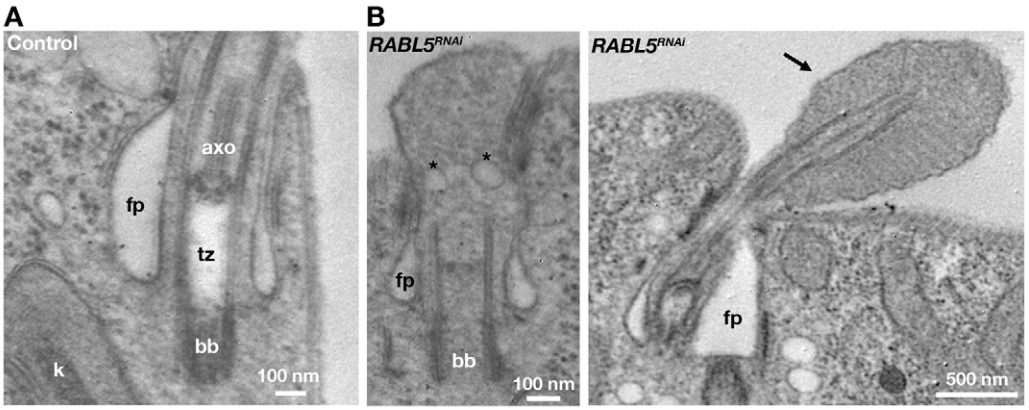


**Fig. 7.** Flagella of *RABL5*$^{RNAi}$ accumulate IFT-like material. Transmission electron micrographs showing the base of the flagellum in control cells (A) and in *RABL5*$^{RNAi}$ cells induced for 4 days (B,C) with bulbous short flagella containing IFT-like material. axo, axoneme; bb, basal body; fp, flagellar pocket; k, kinetoplast; tz, transition zone. Stars indicate the presence of vesicles within a short flagellum, and the arrow points at a short, dilated flagellum emerging from the flagellar pocket.

and mouse models have revealed that mutations in genes involved in Bardet-Biedl syndrome did not have the same structural consequences on all types of cilia (Davis et al., 2007). The results reported here show that radical phenotypic variation can be observed for a conserved ciliary protein and emphasise the importance of analysing carefully the function of these proteins in different contexts and in different model organisms.

## Materials and Methods

### Gene sequences

The *T. brucei* RABL5 protein sequence (XP_829740.1 or Gene DB id Tb11.01.8590) was compared with that of several other organisms: *T. cruzi*, the South American trypanosome, responsible for Chagas disease XP_805503.1; *Leishmania major* (XP_001685647.1), *L. infantum* (XP_001468015.1) and *L. braziliensis* (XP_001567701.1); the divergent protist *Giardia lamblia* (XP_001708211.1); the ciliate *Paramecium tetraurelia*, in which two different protein-coding genes were identified (XP_001458678.1 and XP_001461610.1); the green algae *Chlamydomonas reinharditii* (XP_001689669.1); the nematodes *C. elegans* (NP_503073.1) and *C. briggsae* (XP_001666841.1); and several vertebrates such as human (NP_073614.1), mouse (NP_080349.1 and AAH09150.1), rat (NP_001011902.1), dog (XP_536853.2), cow (NP_001015612.1), opossum (XP_001366207.1) and zebrafish (NP_001017884.1).

### Trypanosome cell lines and cultures

*T. brucei* cell lines were derivatives of strain 427 and grown in SDM79 medium with hemin and 10% foetal calf serum. The 29-13 cell line expressing the T7 RNA polymerase and the tetracycline-repressor (Wirtz et al., 1999) has been described previously, as well as the RNAi cell lines *IFT88*$^{RNAi}$ (Kohl et al., 2003), *IFT140*$^{RNAi}$ and *IFT172*$^{RNAi}$ (Absalon et al., 2008b).

### Plasmid construction and transformation in trypanosomes

For generation of the *RABL5*$^{RNAi}$ cell line, a 447 nucleotide fragment of *RABL5* was cloned in the pZJM vector (Wang et al., 2000), allowing for tetracycline-inducible expression of dsRNA generating RNAi upon transfection in the 29-13 recipient cell line. The dsRNA is expressed from two tetracycline-inducible T7 promoters facing each other in the pZJM vector. Primers were selected using the RNAit algorithm to ensure that the fragment lacked significant identical residues to other genes to avoid cross-RNAi (Redmond et al., 2003). The fragment was amplified by PCR using primers CGATCGAAGCTTGGATAGTCTTTTGCTTC and GTCATCTCGAGCGCGGATAG TCTTTTGCTTC from *T. brucei* genomic DNA, digested with *Hin*dIII and *Xho*I (restriction sites underlined) and ligated in the corresponding sites of the pZJM vector. The pZJMRABL5 plasmid was linearized with *Not*I and transformed in 29-13 cells. Transfected cells were immediately cloned and antibiotic-resistant cell lines obtained. RNAi was induced by addition of 1 μg tetracycline per ml of medium and fresh tetracycline was added at each cell dilution. For generation of GFP::RABL5, the full-length *RABL5* gene was amplified by PCR with the proof-reading enzyme *Pfu*I using GCATCAGATATCATGTCGGACGACTTGGTAAAG (*Eco*RV site underlined) and GCATCGGATATCTCAACGCTTCAGCCGCG-GATAGTC (*Eco*RV site underlined) and ligated into the pPCPFR plasmid digested with *Eco*RV (Sabrina Absalon and P.B., Institut Pasteur, Paris, unpublished results). The eGFP gene was amplified by PCR with the proofreading enzyme *Pfu*I using GCATCAAAGCTTATGGTGAGCAAGGGCGAG (*Hin*dIII site underlined) and GCATCGAAGCTTCTTGTACAGCTCCGTCCAT (*Hin*dIII site underlined) and then ligated into the pPCPFRRABL5 plasmid to generate pPCPFReGFPRABL5. This plasmid was linearized by *Nsi*I and integrated in the intergenic region of *PFR2*. Inserted sequences and flanking regions were sequenced to confirm correct fusion (Genome express). Transfected cells were immediately cloned and all antibiotic-resistant cell lines characterized by direct fluorescence.

### Protein expression and antibody production

Full-length RABL5 amplified with the *Pfu*I proofreading enzyme, using GCATCAGAATTCATGTCGGACGACTTGGTAAAG (*Eco*RI site underlined) and GCATCGAAGCTTTCAACGCTTCAGCCGCGGATAGTC (*Hin*dIII site underlined) was digested with *Eco*RI and *Hin*dIII, and ligated in compatible sites of the pGEXB vector. The plasmid was sequenced to confirm correct fusion with GST and transformed in *E. coli* BL21. Protein expression was analyzed by SDS-polyacrylamide gel electrophoresis (PAGE) followed by Coomassie staining. Glutathione transferase (GST)-coupled proteins were purified as described previously (Smith and Johnson, 1988) and 20 μg were administrated by four successive subcutaneous injections (every 3 weeks) to BALB/c mice for immunization. After bleeding, sera were absorbed against GST. Sera from mice immunized with GST alone were used as negative controls.

### Immunofluorescence

For IFA with anti-RABL5 antisera, intact cells or detergent-extracted cytoskeletons were washed, settled on poly-L-lysine-coated slides and fixed in methanol (–20°C) for 5 minutes. For detergent treatment, cells were settled on poly-L-lysine coated slides and exposed to 1% Nonidet P-40 in spindle stabilisation buffer [4 M glycerol, 5 mM EGTA, 10 mM $MgCl_2$, 10 mM PIPES and 0.1% (v/v) Triton X-100 (pH 6.5)]. Blocking was performed for 45-60 minutes in PBS containing 1% bovine serum albumin and washed slides were incubated with anti-RABL5 antisera for 45-60 minutes. Slides were washed and incubated with anti-mouse secondary antibodies coupled to FITC (Sigma). Other antibodies used are L8C4, a marker of flagellum assembly (Kohl et al., 1999); MAb22 a marker of both the mature and the pro-basal body; and MAb25, which recognises a protein found all along the axoneme (Bonhivers et al., 2008; Absalon et al., 2007; Pradel et al., 2006) and mouse polyclonal antisera raised against a GST::IFT172 or a GST::PIFTF6 fusion protein (C.A., T.B., G.T., E.D. and P.B., unpublished). GFP was observed directly or upon IFA using an anti-GFP antibody (Invitrogen). Subclass-specific secondary antibodies coupled to FITC (Sigma), Alexa 488 or Alexa 594 (Invitrogen), Cy3 or Cy5 (Jackson) were used for double labelling. For visualization of GFP, live cells were mixed with a solution of 3% LMP agarose (Biorad) to reduce cell movement. Samples were observed with a DMR Leica microscope and images were captured with a Cool Snap HQ camera (Roper Scientific). Images were analysed using the IPLab Spectrum 3.9 software (Scanalytics & BD Biosciences).

### Electron microscopy

Transmission (Branche et al., 2006) and scanning (Absalon et al., 2007) electron microscopy were carried out exactly as previously described.

### RT-PCR

Total RNA was extracted using Trizol from cells grown with or without tetracycline for the indicated periods of time. DNA was eliminated by DNase treatment and RNA purity was confirmed by conventional PCR. For determination of optimal conditions for RT-PCR, 10-2000 ng template total RNA from wild-type trypanosomes were incubated with 0.8 μM primers and amplified by the mean of the RT-Taq Platinum (Invitrogen) enzyme mix to find out the linear range of the reaction. Appropriate temperature for annealing was determined using a temperature gradient on a DNA Engine (BioRad) PCR machine. Once these parameters were established, 100 ng of RNA from induced and non-induced *RABL5*$^{RNAi}$ cells was used for semi-quantitative RT-PCR performed as described (Durand-Dubief et al., 2003). To assess the extent of RNAi silencing in induced samples, up to 2 μg RNA were used. Primers used were ATGTCGGACGACTTGGTAAAG (forward) and TCAACGCTTCAG-CCGCGGATAG (reverse). They are outside the region selected for dsRNA and encompass the full coding sequence.

### Western blot

Cells ($1\times10^6$/µl) were washed in PBS and boiled in gel sample buffer before SDS-PAGE. Proteins were transferred to PVDF membranes and incubated with a 1:500 dilution of anti-RABL5. Membranes were stripped and probed with the anti-PFR antibody L13D6 (Kohl et al., 1999) or with a rabbit anti-Bip antibody (Bangs et al., 1993) as loading control and revealed with ECL+ (Amersham).

We acknowledge Derrick Robinson and Mélanie Bonhivers (Bordeaux) for generous gifts of numerous monoclonal antibodies, the electron microscopy department of the Muséum National d'Histoire Naturelle for providing access to their equipment and Joel Rosenbaum for thorough comments on the manuscript. We also thank Derrick Robinson for critical reading of the manuscript. C.A. was funded by an FRM postdoctoral fellowship. This work was funded by the Pasteur Institute, the CNRS and by Fonds Dédié Sanofi-Aventis/Ministère de la Recherche 'Combattre les Maladies Parasitaires'.

## References

**Absalon, S., Kohl, L., Branche, C., Blisnick, T., Toutirais, G., Rusconi, F., Cosson, J., Bonhivers, M., Robinson, D. and Bastin, P.** (2007). Basal body positioning is controlled by flagellum formation in trypanosoma brucei. *PLoS ONE* **2**, e437.

**Absalon, S., Blisnick, T., Bonhivers, M., Kohl, L., Cayet, N., Toutirais, G., Buisson, J., Robinson, D. R. and Bastin, P.** (2008a). Flagellum elongation is required for correct structure, orientation and function of the flagellar pocket in *Trypanosoma brucei*. *J. Cell Sci.* **121**, 3704-3716.

**Absalon, S., Blisnick, T., Kohl, L., Toutirais, G., Dore, G., Julkowska, D., Tavenet, A. and Bastin, P.** (2008b). Intraflagellar transport and functional analysis of genes required for flagellum formation in trypanosomes. *Mol. Biol. Cell* **19**, 929-944.

**Avidor-Reiss, T., Maer, A. M., Koundakjian, E., Polyanovsky, A., Keil, T., Subramaniam, S. and Zuker, C. S.** (2004). Decoding cilia function: defining specialized genes required for compartmentalized cilia biogenesis. *Cell* **117**, 527-539.

**Bangs, J. D., Uyetake, L., Brickman, M. J., Balber, A. E. and Boothroyd, J. C.** (1993). Molecular cloning and cellular localization of a BiP homologue in Trypanosoma brucei: divergent ER retention signals in a lower eukaryote. *J. Cell Sci.* **105**, 1101-1113.

**Baron, D. M., Ralston, K. S., Kabututu, Z. P. and Hill, K. L.** (2007). Functional genomics in Trypanosoma brucei identifies evolutionarily conserved components of motile flagella. *J. Cell Sci.* **120**, 478-491.

**Blacque, O. E., Li, C., Inglis, P. N., Esmail, M. A., Ou, G., Mah, A. K., Baillie, D. L., Scholey, J. M. and Leroux, M. R.** (2006). The WD repeat-containing protein IFTA-1 is required for retrograde intraflagellar transport. *Mol. Biol. Cell* **17**, 5053-5062.

**Bonhivers, M., Landrein, N., Decossas, M. and Robinson, D. R.** (2008). A monoclonal antibody marker for the exclusion-zone filaments of Trypanosoma brucei. *Parasit. Vectors* **1**, 21.

**Branche, C., Kohl, L., Toutirais, G., Buisson, J., Cosson, J. and Bastin, P.** (2006). Conserved and specific functions of axoneme components in trypanosome motility. *J. Cell Sci.* **119**, 3443-3455.

**Briggs, L. J., Davidge, J. A., Wickstead, B., Ginger, M. L. and Gull, K.** (2004). More than one way to build a flagellum: comparative genomics of parasitic protozoa. *Curr. Biol.* **14**, R611-R612.

**Broadhead, R., Dawe, H. R., Farr, H., Griffiths, S., Hart, S. R., Portman, N., Shaw, M. K., Ginger, M. L., Gaskell, S. J., McKean, P. G. et al.** (2006). Flagellar motility is required for the viability of the bloodstream trypanosome. *Nature* **440**, 224-227.

**Cole, D. G.** (2003). The intraflagellar transport machinery of Chlamydomonas reinhardtii. *Traffic* **4**, 435-442.

**Cole, D. G., Diener, D. R., Himelblau, A. L., Beech, P. L., Fuster, J. C. and Rosenbaum, J. L.** (1998). Chlamydomonas kinesin-II-dependent intraflagellar transport (IFT): IFT particles contain proteins required for ciliary assembly in Caenorhabditis elegans sensory neurons. *J. Cell Biol.* **141**, 993-1008.

**Cuvillier, A., Redon, F., Antoine, J. C., Chardin, P., DeVos, T. and Merlin, G.** (2000). LdARL-3A, a Leishmania promastigote-specific ADP-ribosylation factor-like protein, is essential for flagellum integrity. *J. Cell Sci.* **113**, 2065-2074.

**Davidge, J. A., Chambers, E., Dickinson, H. A., Towers, K., Ginger, M. L., McKean, P. G. and Gull, K.** (2006). Trypanosome IFT mutants provide insight into the motor location for mobility of the flagella connector and flagellar membrane formation. *J. Cell Sci.* **119**, 3935-3943.

**Davis, R. E., Swiderski, R. E., Rahmouni, K., Nishimura, D. Y., Mullins, R. F., Agassandian, K., Philp, A. R., Searby, C. C., Andrews, M. P., Thompson, S. et al.** (2007). A knockin mouse model of the Bardet-Biedl syndrome 1 M390R mutation has cilia defects, ventriculomegaly, retinopathy, and obesity. *Proc. Natl. Acad. Sci. USA* **104**, 19422-19427.

**Durand-Dubief, M., Kohl, L. and Bastin, P.** (2003). Efficiency and specificity of RNA interference generated by intra- and intermolecular double stranded RNA in Trypanosoma brucei. *Mol. Biochem. Parasitol.* **129**, 11-21.

**Fan, Y., Esmail, M. A., Ansley, S. J., Blacque, O. E., Boroevich, K., Ross, A. J., Moore, S. J., Badano, J. L., May-Simera, H., Compton, D. S. et al.** (2004). Mutations in a member of the Ras superfamily of small GTP-binding proteins causes Bardet-Biedl syndrome. *Nat. Genet.* **36**, 989-993.

**Follit, J. A., Tuft, R. A., Fogarty, K. E. and Pazour, G. J.** (2006). The intraflagellar transport protein IFT20 is associated with the Golgi complex and is required for cilia assembly. *Mol. Biol. Cell* **17**, 3781-3792.

**Kohl, L. and Bastin, P.** (2005). The Flagellum of Trypanosomes. In *International Review of Cytology*, vol. 244, pp. 227-285. New York: Academic Press.

**Kohl, L., Sherwin, T. and Gull, K.** (1999). Assembly of the paraflagellar rod and the flagellum attachment zone complex during the Trypanosoma brucei cell cycle. *J. Eukaryot. Microbiol.* **46**, 105-109.

**Kohl, L., Robinson, D. and Bastin, P.** (2003). Novel roles for the flagellum in cell morphogenesis and cytokinesis of trypanosomes. *EMBO J.* **22**, 5336-5346.

**Krock, B. L. and Perkins, B. D.** (2008). The intraflagellar transport protein IFT57 is required for cilia maintenance and regulates IFT-particle-kinesin-II dissociation in vertebrate photoreceptors. *J. Cell Sci.* **121**, 1907-1915.

**Li, J. B., Gerdes, J. M., Haycraft, C. J., Fan, Y., Teslovich, T. M., May-Simera, H., Li, H., Blacque, O. E., Li, L., Leitch, C. C. et al.** (2004). Comparative genomics identifies a flagellar and basal body proteome that includes the BBS5 human disease gene. *Cell* **117**, 541-552.

**Marshall, W. F.** (2008). The cell biological basis of ciliary disease. *J. Cell Biol.* **180**, 17-21.

**Mukhopadhyay, S., Lu, Y., Qin, H., Lanjuin, A., Shaham, S. and Sengupta, P.** (2007). Distinct IFT mechanisms contribute to the generation of ciliary structural diversity in C. elegans. *EMBO J.* **26**, 2966-2980.

**Omori, Y., Zhao, C., Saras, A., Mukhopadhyay, S., Kim, W., Furukawa, T., Sengupta, P., Veraksa, A. and Malicki, J.** (2008). Elipsa is an early determinant of ciliogenesis that links the IFT particle to membrane-associated small GTPase Rab8. *Nat. Cell Biol.* **10**, 437-444.

**Ou, G., Koga, M., Blacque, O. E., Murayama, T., Ohshima, Y., Schafer, J. C., Li, C., Yoder, B. K., Leroux, M. R. and Scholey, J. M.** (2007). Sensory ciliogenesis in Caenorhabditis elegans: assignment of IFT components into distinct modules based on transport and phenotypic profiles. *Mol. Biol. Cell* **18**, 1554-1569.

**Pazour, G. J., Dickert, B. L. and Witman, G. B.** (1999). The DHC1b (DHC2) isoform of cytoplasmic dynein is required for flagellar assembly. *J. Cell Biol.* **144**, 473-481.

**Pazour, G. J., Agrin, N., Leszyk, J. and Witman, G. B.** (2005). Proteomic analysis of a eukaryotic cilium. *J. Cell Biol.* **170**, 103-113.

**Piperno, G., Mead, K. and Henderson, S.** (1996). Inner dynein arms but not outer dynein arms require the activity of kinesin homologue protein KHP1(FLA10) to reach the distal part of flagella in Chlamydomonas. *J. Cell Biol.* **133**, 371-379.

**Porter, M. E., Bower, R., Knott, J. A., Byrd, P. and Dentler, W.** (1999). Cytoplasmic dynein heavy chain 1b is required for flagellar assembly in Chlamydomonas. *Mol. Biol. Cell* **10**, 693-712.

**Pradel, L. C., Bonhivers, M., Landrein, N. and Robinson, D. R.** (2006). NIMA-related kinase TbNRKC is involved in basal body separation in Trypanosoma brucei. *J. Cell Sci.* **119**, 1852-1863.

**Qin, H., Diener, D. R., Geimer, S., Cole, D. G. and Rosenbaum, J. L.** (2004). Intraflagellar transport (IFT) cargo: IFT transports flagellar precursors to the tip and turnover products to the cell body. *J. Cell Biol.* **164**, 255-266.

**Qin, H., Wang, Z., Diener, D. and Rosenbaum, J.** (2007). Intraflagellar transport protein 27 is a small G protein involved in cell-cycle control. *Curr. Biol.* **17**, 193-202.

**Ralston, K. S. and Hill, K. L.** (2008). The flagellum of Trypanosoma brucei: new tricks from an old dog. *Int. J. Parasitol.* **38**, 869-884.

**Redmond, S., Vadivelu, J. and Field, M. C.** (2003). RNAit: an automated web-based tool for the selection of RNAi targets in Trypanosoma brucei. *Mol. Biochem. Parasitol.* **128**, 115-118.

**Robinson, D. R. and Gull, K.** (1991). Basal body movements as a mechanism for mitochondrial genome segregation in the trypanosome cell cycle. *Nature* **352**, 731-733.

**Rosenbaum, J. L. and Witman, G. B.** (2002). Intraflagellar transport. *Nat. Rev. Mol. Cell. Biol.* **3**, 813-825.

**Schafer, J. C., Winkelbauer, M. E., Williams, C. L., Haycraft, C. J., Desmond, R. A. and Yoder, B. K.** (2006). IFTA-2 is a conserved cilia protein involved in pathways regulating longevity and dauer formation in Caenorhabditis elegans. *J. Cell Sci.* **119**, 4088-4100.

**Scholey, J. M.** (2008). Intraflagellar transport motors in cilia: moving along the cell's antenna. *J. Cell Biol.* **180**, 23-29.

**Sherwin, T. and Gull, K.** (1989). The cell division cycle of Trypanosoma brucei brucei: timing of event markers and cytoskeletal modulations. *Philos. Trans. R. Soc. Lond., B Biol. Sci.* **323**, 573-588.

**Signor, D., Wedaman, K. P., Orozco, J. T., Dwyer, N. D., Bargmann, C. I., Rose, L. S. and Scholey, J. M.** (1999). Role of a class DHC1b dynein in retrograde transport of IFT motors and IFT raft particles along cilia, but not dendrites, in chemosensory neurons of living Caenorhabditis elegans. *J. Cell Biol.* **147**, 519-530.

**Smith, D. B. and Johnson, K. S.** (1988). Single-step purification of polypeptides expressed in *Escherichia coli* as fusions with glutathione S-transferase. *Gene* **67**, 31-40.

**Wang, Z., Morris, J. C., Drew, M. E. and Englund, P. T.** (2000). Inhibition of Trypanosoma brucei gene expression by RNA interference using an integratable vector with opposing T7 promoters. *J. Biol. Chem.* **275**, 40174-40179.

**Wirtz, E., Leal, S., Ochatt, C. and Cross, G. A.** (1999). A tightly regulated inducible expression system for conditional gene knock-outs and dominant-negative genetics in Trypanosoma brucei. *Mol. Biochem. Parasitol.* **99**, 89-101.

**Yang, J., Guo, S. Y., Pan, F. Y., Geng, H. X., Gong, Y., Lou, D., Shu, Y. Q. and Li, C. J.** (2007). Prokaryotic expression and polyclonal antibody preparation of a novel Rab-like protein mRabL5. *Protein Expr. Purif.* **53**, 1-8.

**Yoshimura, S., Egerer, J., Fuchs, E., Haas, A. K. and Barr, F. A.** (2007). Functional dissection of Rab GTPases involved in primary cilium formation. *J. Cell Biol.* **178**, 363-369.

Journal of Cell Science